Theor Chem Acc (2012) 131:1246
DOI 10.1007/s00214-012-1246-3

REGULAR ARTICLE

S_5 graphs as model systems for icosahedral Jahn–Teller problems

A. Ceulemans · E. Lijnen · P. W. Fowler · R. B. Mallion · T. Pisanski

Received: 2 April 2012 / Accepted: 7 June 2012 / Published online: 26 June 2012

Abstract The degeneracy of the eigenvalues of the adjacency matrix of graphs may be broken by non-uniform changes of the edge weights. This symmetry breaking is the graph-theoretical equivalent of the molecular Jahn–Teller effect (Ceulemans et al. in Proc Roy Soc 468:971–989, 2012). It is investigated for three representative graphs, which all have the symmetric group on 5 elements, $\mathbf{S_5}$, as automorphism group: the complete graph K_5, with 5 nodes, the Petersen graph, with 10 nodes, and an extended K_5 graph with 20 nodes. The spectra of these graphs contain fourfold, fivefold, and sixfold degenerate manifolds, respectively, and provide model systems for the study of the Jahn–Teller effect in icosahedral molecules. The $\mathbf{S_5}$ symmetries of the distortion modes of the quintuplet in the Petersen graph yield a resolution of the product multiplicity in the corresponding $H \otimes (g + 2h)$ icosahedral Jahn–Teller problem. In the extended Petersen graph with 20 nodes, a selection rule prevents the Jahn–Teller splitting of the sextuplet into two conjugate icosahedral triplets.

Keywords Jahn–Teller effect · Icosahedral symmetry · $\mathbf{S_5}$ symmetry · Spectral graph-theory · Electronic/spectral degeneracy

Published as part of the special collection of articles celebrating theoretical and computational chemistry in Belgium.

A. Ceulemans (✉) · E. Lijnen
Division of Quantum Chemistry and Physical Chemistry, Department of Chemistry, K. U. Leuven, Celestijnenlaan 200F, 3001 Heverlee, Belgium
e-mail: arnout.ceulemans@chem.kuleuven.be

P. W. Fowler
Department of Chemistry, University of Sheffield, Sheffield S3 7HF, UK

R. B. Mallion
School of Physical Sciences, University of Kent, Canterbury CT2 7NH, UK

T. Pisanski
Faculty of Mathematics and Physics, University of Ljubljana, Jadranska 19, 1000 Ljubljana, Slovenia

1 Introduction

Symmetry may give rise to electronic degeneracy. A molecule in a degenerate state cannot be described by a single wave function. Instead, it will be characterized by a set of eigenfunctions, forming a so-called function space. Any linear combination of eigenfunctions corresponding to a direction in this space is a valid description of the state of the molecule. According to the Jahn–Teller (JT) theorem, this is not a stable situation. While the function space as a whole is an invariant of the molecular symmetry, this is not the case for the individual eigenfunctions. As a result, there will be an imbalance between the symmetric charge distribution of the nuclei and the non-symmetric charge distribution of the electronic state, giving rise to an electric force, which distorts the molecule to a structure of lower symmetry where the degeneracy is lifted [1, 2]. Molecular graphs are concise representations of molecules, which reduce a molecule to a set of atoms or 'nodes' connected by a network of bonds or 'lines' [3]. The graph-theoretical equivalent of the molecular symmetry group is the automorphism group of the graph. The elements of this group are the permutations of nodes that keep the bonding network of the graph intact. The 'states' of the graph correspond to the eigenfunctions and eigenvalues of its adjacency matrix, the latter being the *spectrum* of the graph. These analogies between molecules and graphs have

made us wonder whether there might also exist a graph-theoretical equivalent of the JT theorem. In a previous publication we have formulated the conjecture that *whenever the spectrum of a graph contains a set of non-zero degenerate eigenvalues, the roots of the Hamiltonian matrix over this set will show a linear dependence on edge distortions, which has the effect of lifting the degeneracy* [4]. The derivatives with respect to the distortion modes are the essential coupling parameters. These parameters are graph invariants. The graph-theoretical analogue of the JT theorem will hold whenever these parameters are different from zero. For non-bonding degenerate-eigenlevels, that is, with eigenvalue zero, there will be edge distortions in the active space that cannot couple to the degeneracy and then distortions of the vertex weights must also be included, in order to complete the JT Hamiltonian.

This conjecture has implications in both directions. It extends the notion of distortivity of a graph [5] by relating it to the coupling parameters associated with degeneracies in graph spectra. From the molecular point of view, graphs provide new models for the treatment of JT interactions. In the present article, we shall use the conjecture to study the JT effect for icosahedral orbital degeneracies. Three graphs of increasing complexity will be used in order to model fourfold, fivefold, and pairs of threefold degenerate-states in icosahedra. They are, respectively, the complete graph with five nodes, the Petersen graph, with 10 nodes, and an extended K_5 graph with 20 nodes. The automorphism group of each of these graphs is the symmetric group on five elements, $\mathbf{S_5}$, of order 120. The subgroup of even permutations is the alternating group, $\mathbf{A_5}$, of order 60. The symmetry point group of the icosahedron, $\mathbf{I_h}$, also has 120 elements, but it is not isomorphic to $\mathbf{S_5}$. Its rotational subgroup, $\mathbf{I}$, is, however, isomorphic to $\mathbf{A_5}$. The present treatment relies on this correspondence.

2 S_5 graphs

In Fig. 1 we illustrate the three graphs of increasing sophistication on which the present treatment is based. The smallest graph in Fig. 1a is the fully connected 5-vertex graph, which is the skeleton of the simplex in 4D space. This is the complete graph with 5 vertices, known as K_5. Its automorphism group corresponds to the symmetric group on 5 elements. The corresponding permutations are denoted by their cycle structure. A mapping of type $\{a \to b\}\{b \to a\}\{c \to d\}\{d \to e\}\{e \to c\}$ has two cycles, of length 2 and 3, respectively, and is abbreviated as $(ab)(cde)$. All operations with the same cycle structure belong to the same conjugacy class, which is thus characterized uniquely by the cycle lengths. For the present example this is: {2,3}. For convenience, the character table of this group is reproduced here (Table 1). Irreducible representations (irreps) are denoted by the partitions of 5 cells in a Young tableau [6]. We have also introduced corresponding character labels, based on the icosahedral point group. The letters A, G, H, and I refer to one-, four-, five-, and sixfold degenerate representations, and the subscripts 1 or 2 distinguish representations that are symmetric or antisymmetric with respect to the $\mathbf{A_5}$ subgroup of even permutations. The A_2 irrep is the so-called pseudo-scalar representation. It is symmetric for even permutations and anti-symmetric for odd permutations. Multiplication by A_2 will interchange symmetric and anti-symmetric irreps. Note that all representations occur in pairs, apart from I, which has zero character for the odd permutations, and are thus not affected by multiplication with A_2.

The Petersen graph, shown in Fig. 1b, is a 10-vertex graph, which also has the $\mathbf{S_5}$ automorphism group. In Table 2 we list the corresponding cycle structure for the different $\mathbf{S_5}$ operations, as well as explicit forms of the generators. The Petersen graph is 3-regular and contains 15 edges. All these edges can be permuted into each other by the $\mathbf{S_5}$ operations, and they are therefore said to form a

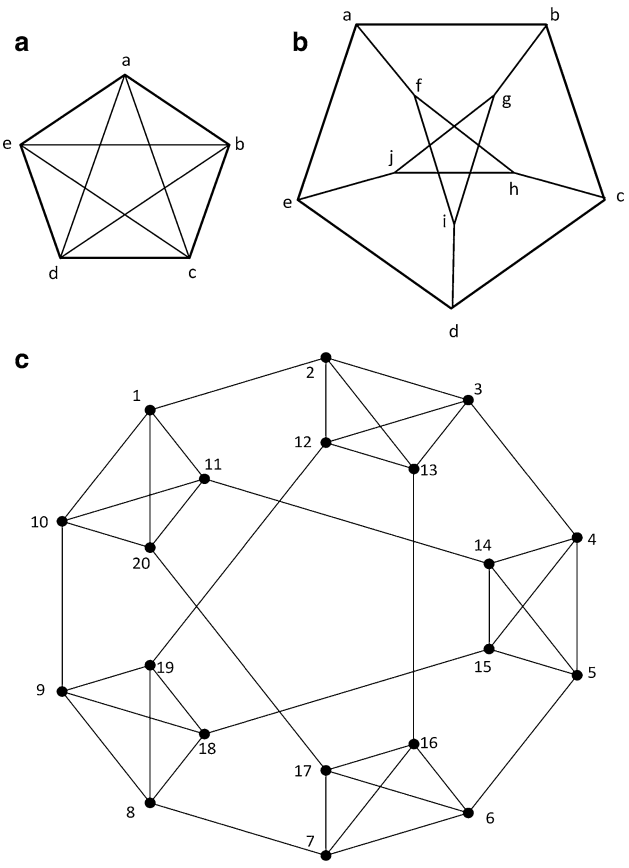

Fig. 1 Three graphs with automorphism group $\mathbf{S_5}$: **a** the complete 5-graph, K_5; **b** the (10-vertex) Petersen graph; **c** an extended K_5 graph with 20 vertices

Table 1 Character table for the symmetric group $\mathbf{S_5}$ and its alternating subgroup $\mathbf{A_5} \sim \mathbf{I}$ with: $\phi = \frac{1}{2}(1+\sqrt{5})$ $-\phi^{-1} = \frac{1}{2}(1-\sqrt{5})$

$\mathbf{S_5}$	$\{1^5\}$ 1	$\{1^3,2\}$ 10	$\{1^2,3\}$ 20	$\{1,2^2\}$ 15	$\{1,4\}$ 30	$\{2,3\}$ 20	$\{5\}$ 24
A_1 (5)	1	1	1	1	1	1	1
G_1 (4,1)	4	2	1	0	0	−1	−1
H_1 (3,2)	5	1	−1	1	−1	1	0
I (3,1^2)	6	0	0	−2	0	0	1
H_2 (2^2,1)	5	−1	−1	1	1	−1	0
G_2 (2,1^3)	4	−2	1	0	0	1	−1
A_2 (1^5)	1	−1	1	1	−1	−1	1

$\mathbf{A_5}$ $\mathbf{I}$	$\{1^5\}$ E 1	$\{1^2,3\}$ C_3 20	$\{1,2^2\}$ C_2 15	$\{5\}$ C_5 12	$\{5\}$ C_5^2 12
A	1	1	1	1	1
G	4	1	0	−1	−1
H	5	−1	1	0	0
T_1	3	0	−1	φ	$-\varphi^{-1}$
T_2	3	0	−1	$-\varphi^{-1}$	φ

Table 2 Cycle structure and generators for the Petersen graph

Class dimension	$\mathbf{S_5}$	Petersen	
1	$\{1^5\}$	$\{1^{10}\}$	(a)(b)(c)(d)(e)(f)(g)(h)(i)(j)
10	$\{1^3,2\}$	$\{1^4,2^3\}$	(a)(b)(c)(g)(ef)(dh)(ij)
20	$\{1^2,3\}$	$\{1,3^3\}$	(a)(efb)(dhg)(cji)
15	$\{1,2^2\}$	$\{1^2,2^4\}$	(a)(f)(be)(cd)(gj)(hi)
30	$\{1,4\}$	$\{2,4^2\}$	(ch)(agei)(bjdf)
20	$\{2,3\}$	$\{1,3,6\}$	(a)(efb)(gjhcdi)
24	$\{5\}$	$\{5^2\}$	(abcde)(fghij)

transitive set or an orbit. The Petersen graph is non-planar, which means that it cannot be drawn in the plane or on the surface of a sphere without intersections. It can, however, be mapped onto a projective plane.

A further graph with $\mathbf{S_5}$ symmetry is the 20-vertex graph shown in Fig. 1c. This graph is obtained as an extension of K_5 [7]. A comparison between K_5 and the 20-vertex graph shows that the original nodes of the complete graph K_5 are replaced, or 'truncated', by copies of K_4. In Table 3 we describe the corresponding cycle structure and generators. This graph is 4-regular and contains 40 edges. In contrast to the previous graphs, these edges form two separate orbits, an orbit of order 10 and an orbit of order 30. The edges of the five K_4 subgraphs form the 30-edge orbit, while the 10 remaining edges correspond to the original connectivity of the K_5 parent graph.

Table 3 Cycle structure and generators for the 20-graph

Class dimension	$\mathbf{S_5}$	20-graph	
1	$\{1^5\}$	$\{1^{20}\}$	(1)(2)…(20)
10	$\{1^3,2\}$	$\{1^6,2^7\}$	(1)(2)(13)(16)(17)(20)(3,12)(4,19)(5,8)(6,7)(9,14)(10,11)(15,18)
20	$\{1^2,3\}$	$\{1^2,3^6\}$	(15)(18)(1,17,13)(2,20,16)(3,11,6)(4,14,5)(10,7,12)
15	$\{1,2^2\}$	$\{2^{10}\}$	(1,10)(2,9)(3,8)(4,7)(5,6)(11,20)(12,19)(13,18)(14,17)(15,16)
30	$\{1,4\}$	$\{4^5\}$	(1,16,4,19)(2,13,3,12)(11,7,14,8)(10,17,5,18)(20,6,15,9)
20	$\{2,3\}$	$\{2,3^2,6^2\}$	(15,18) (1,13,17)(2,16,20)(3,7,11,12,6,10) (4,8,14,19,5,9)
24	$\{5\}$	$\{5^4\}$	(1,3,5,7,9)(10,2,4,6,8)(11,13,15,17,19)(20,12,14,16,18)

3 The complete 5-vertex graph K_5 and the fourfold degeneracy

The group of icosahedral rotations contains a maximal subgroup of tetrahedral rotations, **T**, describing rotations that leave an inscribed cube invariant. Euclid's construction of the dodecahedron is based on this relationship [8]. The ratio of the orders of the groups **I** and **T** is 60/12 = 5. Five different cubes can thus be inscribed. This set of cubes is doubly transitive, that is, there always exists a symmetry operation in the group that can map any ordered pair of elements of the set onto any other ordered pair. Clearly, the five elements of a doubly transitive set will thus correspond to the vertices of K_5. The spectrum of an n-vertex complete graph has one totally symmetric non-degenerate root, with eigenvalue $n-1$, while the remaining roots form a $(n-1)$-fold degenerate irrep, with eigenvalue -1. The graph spectrum is denoted $\left\{(n-1),(-1)^{n-1}\right\}$. The spectrum of K_5 thus contains a fourfold degenerate G representation, which may stand as a model for the icosahedral fourfold degenerate representation. The $G \otimes (g+h)$ Hamiltonian for this manifold has been described previously, and its relationship to the $\mathbf{S_5}$ graph has also been demonstrated [9, 10]. We briefly recapitulate the results. To apply the graph-theoretical JT theorem, we start from the eigenvectors associated with the -1 roots. They appear as

linear combinations of the five nodes. Each node will be presented by a ket symbol. The kth eigenvector is given by:

$$|k> = \sum_{i=1}^{n} c_i^k |i> \tag{1}$$

In case of the orbital quadruplet, the components of the function space are labeled as (a,x,y,z) following the Boyle and Parker conventions [11]. The vertices are labeled as in Fig. 1a. The orthonormal form of the function space is given by:

$$\begin{aligned}
|Ga> &= \frac{1}{2\sqrt{5}}(4|a> - |b> - |c> - |d> - |e>) \\
|Gx> &= \frac{1}{2}(-|b> + |c> - |d> + |e>) \\
|Gy> &= \frac{1}{2}(|b> - |c> - |d> + |e>) \\
|Gz> &= \frac{1}{2}(-|b> - |c> + |d> + |e>)
\end{aligned} \tag{2}$$

The operator corresponding to the linear JT Hamiltonian is expressed as:

$$H = \sum_{i<j} \gamma \Delta r_{ij}(|i><j| + |j><i|) \tag{3}$$

Here, γ is a constant factor, corresponding to the first-order distance-derivative of the interaction-matrix element. The JT interaction matrix is obtained by acting with this operator in the function space. In general:

$$H_{kl} = \sum_i \sum_j \gamma \Delta r_{ij}\left(c_i^k c_j^l + c_j^k c_i^l\right) \tag{4}$$

As we have shown elsewhere, the coefficients in this expression correspond to the elements of the bond-order matrix [4]. Because the JT Hamiltonian is Hermitian and invariant under time reversal, it is represented by a symmetric matrix in a real function space. The symmetries of this interaction matrix will therefore correspond to the symmetrized direct square of the degenerate irrep of the function space. This part of the direct square is represented by square brackets. The corresponding character is given by [8]:

$$\chi^{[\Gamma]^2}(R) = \frac{1}{2}\left(\left(\chi^{\Gamma}(R)\right)^2 + \chi^{\Gamma}(R^2)\right) \tag{5}$$

In Table 4, we show how this applies to the direct square of the G representation. It reduces as follows:

$$[G \otimes G] = A_1 + G_1 + H_1 \tag{6}$$

The A_1 component is totally symmetric and cannot change the symmetry, but the G + H part of the interaction matrix contains the JT-active modes. On the other hand, the distortion space of the graph corresponds to the elongations and contractions of its edges (i.e., a decrease or increase in the weights of its edges). The automorphism group of the graph maps edges onto edges, which implies that the symmetry of the distortion space is given by the edge representation, denoted as Γ_e. Character reduction shows that the 10 edges transform in exactly the same way as the $[G \otimes G]$ symmetrized square. Hence, in the $\mathbf{S_5}$ graph the edge distortions, minus the totally symmetric component, coincide exactly with the JT modes that will lift the quadruplet degeneracy. This result can be shown to be true for every complete graph [10]. Indeed, in general, the edge representation can be obtained by forming the symmetrized square of the vertex representation, Γ_v. As mentioned earlier, for K_5 this vertex representation contains the totally symmetric component and an $(n-1)$-fold degenerate irrep:

$$\Gamma_v = \Gamma_0 + \Gamma_{n-1} \tag{7}$$

The edges are formed by all pairwise combinations of vertices, omitting self-interactions. The latter interactions transform as Γ_v. The edge symmetries thus precisely correspond to the symmetrized square of Γ_v minus the on-site representation:

$$\begin{aligned}
\Gamma_e &= [\Gamma_v \otimes \Gamma_v] - \Gamma_v \\
&= [(\Gamma_0 + \Gamma_{n-1}) \otimes (\Gamma_0 + \Gamma_{n-1})] - \Gamma_v \\
&= [\Gamma_{n-1} \otimes \Gamma_{n-1}]
\end{aligned} \tag{8}$$

The full Hamiltonian for the G-state in the graph has been given elsewhere [9]. The molecular JT problem has two minimal-energy solutions: one tetrahedral along the G-distortion, and one trigonal, along a combination of G and H. The corresponding coupling constants depend on the

Table 4 Derivation of the characters for the symmetrized direct square $[G \otimes G]$ in $\mathbf{S_5}$

G	$\{1^5\}$ 1	$\{1^3,2\}$ 10	$\{1^2,3\}$ 20	$\{1,2^2\}$ 15	$\{1,4\}$ 30	$\{2,3\}$ 20	$\{5\}$ 24
χ(R)	4	2	1	0	0	−1	−1
χ^2(R)	16	4	1	0	0	1	1
χ(R^2)	4	4	1	4	0	1	−1
[G × G]	10	4	1	2	0	1	0

The final row is the average of the two preceding rows (see Eq. 5)

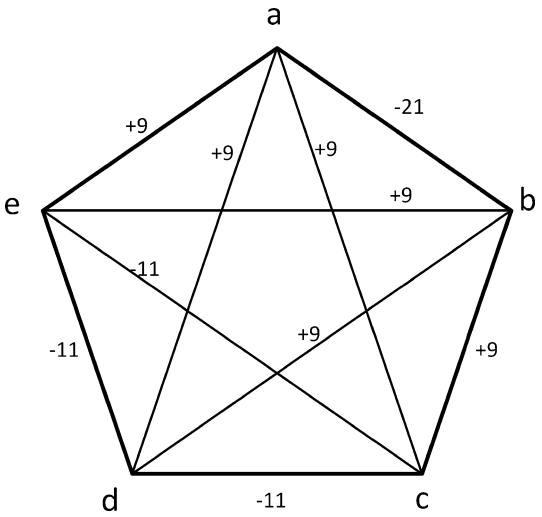

Fig. 2 Edge distortions of the complete graph K_5 that lead to an absolute trigonal minimum (unnormalized)

detailed nature of the molecular interactions. However, in a graph there is only one fundamental constant, γ, which implies that the ratio of the coupling constants for the different distortion modes will be fixed. For K_5, the respective slopes are $-\sqrt{3/5}\,\gamma \approx -0.775\,\gamma$ for the tetrahedral distortion, versus $-\sqrt{3/2}\,\gamma \approx -1.225\,\gamma$ for the trigonal distortion. Hence, the most efficient way to lift the degeneracy of this graph is by means of a trigonal distortion. The threefold symmetry is directed along one of the ten edges. Ten equivalent trigonal distortion paths thus exist. One of these is represented in Fig. 2. The map that connects adjacent minima is precisely the Petersen graph [9].

4 The Petersen graph and the fivefold degeneracy

The group of icosahedral rotations also contains a maximal pentagonal subgroup, $\mathbf{D_5}$, which leaves a pentagonal antiprism invariant. The ratio of group orders is $60/10 = 6$, corresponding to the presence of six pentagonal directions. This set of six is also doubly transitive and therefore gives rise to a fivefold degenerate representation, which is the highest orbital degeneracy of the point groups. This quintuplet will appear in the spectrum of the fully connected graph on six elements, with the symmetric group $\mathbf{S_6}$ as automorphism group. In the same way as the quadruplet was related to K_5, the K_6-graph offers a model for analyzing the JT activity of the quintuplet. The connection is based on a special embedding of $\mathbf{I}$ in $\mathbf{S_6}$ and has been elaborated in previous contributions [2, 10]. At present, we propose a different model for the quintuplet symmetry breaking, using $\mathbf{S_5}$ instead of $\mathbf{S_6}$. For this purpose we investigate the 10-vertex Petersen graph. Its automorphism group is isomorphic with the symmetric group $\mathbf{S_5}$ on 5 objects, but in addition, it has a fivefold degenerate root. The graph spectrum is $\left\{3, 1^5, (-2)^4\right\}$. The Petersen graph is thus an example of an integral graph, one that has only integer eigenvalues. The 10 vertices of the Petersen graph can be shown to transform as:

$$\Gamma_v = A_1 + G_1 + H_1 \tag{9}$$

As was already mentioned in the previous section, the Petersen graph provides a map of the space of trigonal distortions of an icosahedron. Such distortions arise not only in the quadruplet but also in the quintuplet problem. Since the spectrum has both G and H states, tunneling ground states of the dynamic JT problem can have A, G, or H symmetries, and this may give rise to different JT dynamics [12]. The present section studies the H_1 state of the Petersen graph, which corresponds to the orbital quintuplet. If each node provides one electron, the fivefold degenerate level at $E = 1$ will host 8 electrons. The JT problem is thus concerned with distributing four electron pairs over five orbitals. The JT active modes can be identified by taking the symmetrized product of this representation minus the totally symmetric irrep.

$$[H_1 \otimes H_1] - A_1 = G_1 + H_1 + H_2 \tag{10}$$

The fifteen edges transform as:

$$\Gamma_e = A_1 + G_1 + H_1 + H_2, \tag{11}$$

which indicates that the edge distortions again correspond exactly with the JT-active modes plus the totally symmetric component. The subsequent analysis is based on the general treatment of the $H \otimes (g + 2h)$ JT Hamiltonian [13]. It starts with a symmetry adaptation of the five eigenvectors of our orbital quintuplet.

$$\begin{aligned}
|\theta\rangle &= \frac{1}{2\sqrt{3}}(-|b\rangle + 2|c\rangle - 2|d\rangle + |e\rangle + |h\rangle - |i\rangle) \\
|\varepsilon\rangle &= \frac{1}{2}(|b\rangle + |e\rangle - |h\rangle - |i\rangle) \\
|\xi\rangle &= \frac{1}{\sqrt{6}}(|a\rangle - |b\rangle + |f\rangle - |g\rangle - |h\rangle + |j\rangle) \\
|\eta\rangle &= \frac{1}{\sqrt{6}}(|a\rangle - |e\rangle + |f\rangle + |g\rangle - |i\rangle - |j\rangle) \\
|\zeta\rangle &= \frac{1}{\sqrt{6}}(-|a\rangle - |c\rangle - |d\rangle + |f\rangle + |g\rangle + |j\rangle)
\end{aligned} \tag{12}$$

A general eigenstate of the Hamiltonian can now be represented as:

$$|\Psi\rangle = \theta|\theta\rangle + \varepsilon|\varepsilon\rangle + \xi|\xi\rangle + \eta|\eta\rangle + \zeta|\zeta\rangle \tag{13}$$

with five normalized c-coefficients:

$$\theta^2 + \varepsilon^2 + \xi^2 + \eta^2 + \zeta^2 = 1 \tag{14}$$

Since the orbital quintuplet has eigenvalue different from zero, the full JT Hamiltonian can be expressed solely as a

Table 5 Normalized JT-active modes for the $H_1 \otimes (G_1 + H_1 + H_2)$ problem

	ab	*ae*	*af*	*cd*	*hj*	*ig*	*bg*	*de*	*fh*	*if*	*ej*	*bc*	*di*	*ch*	*gj*
Q_{G_1}															
$3\sqrt{10} \times Q_1$	2	2	2	2	2	2	−3	−3	−3	−3	−3	−3	2	2	2
$\sqrt{6} \times Q_2$	0	0	0	0	0	0	1	1	1	−1	−1	−1	0	0	0
$3\sqrt{2} \times Q_3$	1	−2	1	1	1	−2	0	0	0	0	0	0	1	−2	1
$\sqrt{6} \times Q_4$	1	0	−1	−1	1	0	0	0	0	0	0	0	1	0	−1
Q_{H_1}															
$3\sqrt{2} \times Q_5$	2	2	2	−1	−1	−1	0	0	0	0	0	0	−1	−1	−1
$4 \times Q_6$	0	0	0	1	1	−2	−1	0	1	−1	0	1	−1	2	−1
$4\sqrt{3} \times Q_7$	0	0	0	3	−3	0	−1	2	−1	1	−2	1	3	0	−3
$12 \times Q_8$	2	−4	2	−1	−1	2	3	−6	3	3	−6	3	−1	2	−1
$4\sqrt{3} \times Q_9$	2	0	−2	1	−1	0	3	0	−3	−3	0	3	−1	0	1
Q_{H_2}															
$\sqrt{6} \times Q_{10}$	0	0	0	1	1	1	0	0	0	0	0	0	−1	−1	−1
$4\sqrt{3} \times Q_{11}$	0	0	0	1	1	−2	3	0	−3	3	0	−3	−1	2	−1
$4 \times Q_{12}$	0	0	0	1	−1	0	1	−2	1	−1	2	−1	1	0	−1
$4\sqrt{3} \times Q_{13}$	2	−4	2	−1	−1	2	−1	2	−1	−1	2	−1	−1	2	−1
$4 \times Q_{14}$	2	0	−2	1	−1	0	−1	0	1	1	0	−1	−1	0	1

function of distortions of the 15 edges. As a 5×5 problem, the traceless JT matrix will contain 14 linearly independent active modes labeled Q_1 up to Q_{14}. Normalized expressions for these modes were derived in such a manner that $\{Q_1, Q_2, Q_3, Q_4\}$, $\{Q_5, Q_6, Q_7, Q_8, Q_9\}$, and $\{Q_{10}, Q_{11}, Q_{12}, Q_{13}, Q_{14}\}$ transform, respectively, as the G_1, H_1, and H_2 irreps of $\mathbf{S_5}$. The results are presented in Table 5. The JT Hamiltonian can be constructed straightforwardly using Eq. 4 and Table 5. In order to find the directions of maximal distortion, we shall follow the method of the iso-stationary function [14]. This method avoids the cumbersome diagonalization of the matrix and immediately leads to the directions of maximal distortion. One first adds to the Hamiltonian an isotropic term, which is proportional to the square of the radius of the active space and, in a molecular context, is called the harmonic restoring potential, V.

$$V = \frac{1}{2}\sum_{i=1}^{14} Q_i^2 \tag{15}$$

The eigenvalue corresponding to the state $|\Psi\rangle$ is given by:

$$E(Q) = V(Q) + \sum_{i,j} c_i c_j H_{ij}(Q) \tag{16}$$

The first term in this equation has a quadratic dependence on Q, whereas the second term has a linear dependence. By minimizing E with respect to the Q's, we thus obtain expressions for the stationary coordinates, $\|Q\|$, as a function of the c-coefficients (in units of γ):

$$\begin{aligned}
\|Q_1\| &= \frac{\sqrt{2}}{9\sqrt{5}}\left[7\theta^2 - 3\varepsilon^2 - 3\xi^2 - 3\eta^2 + 2\zeta^2 + 10\xi\zeta + 10\eta\zeta)\right] \\
\|Q_2\| &= \frac{\sqrt{2}}{3\sqrt{3}}\left[-\xi^2 + \eta^2 + 2\sqrt{3}\theta\varepsilon - 2\xi\zeta + 2\eta\zeta\right] \\
\|Q_3\| &= \frac{\sqrt{2}}{9}\left[-\theta^2 + 3\varepsilon^2 - 2\zeta^2 + 6\xi\eta + 2\xi\zeta + 2\eta\zeta\right] \\
\|Q_4\| &= \frac{2}{3\sqrt{3}}\left[\theta\xi + \theta\eta - 2\theta\zeta - \sqrt{3}\varepsilon\xi + \sqrt{3}\varepsilon\eta\right] \\
\|Q_5\| &= \frac{1}{9\sqrt{2}}\left[-\theta^2 + 3\varepsilon^2 - 2\zeta^2 - 6\xi\eta + 2\xi\zeta + 2\eta\zeta\right] \\
\|Q_6\| &= \frac{1}{3\sqrt{2}}\left[\theta\xi - \theta\eta - \sqrt{3}\varepsilon\xi - \sqrt{3}\varepsilon\eta\right] \\
\|Q_7\| &= \frac{1}{6\sqrt{3}}\left[\xi^2 - \eta^2 - 2\sqrt{3}\theta\varepsilon - 4\xi\zeta + 4\eta\zeta\right] \\
\|Q_8\| &= \frac{1}{18}\left[-5\theta^2 - 3\varepsilon^2 + 3\xi^2 + 3\eta^2 + 2\zeta^2 + 4\xi\zeta + 4\eta\zeta\right] \\
\|Q_9\| &= \frac{1}{3\sqrt{6}}\left[-\theta\xi - \theta\eta - 4\theta\zeta + \sqrt{3}\varepsilon\xi - \sqrt{3}\varepsilon\eta\right] \\
\|Q_{10}\| &= \frac{1}{3}\left[\sqrt{3}\theta\xi - \sqrt{3}\theta\eta + \varepsilon\xi + \varepsilon\eta + 2\varepsilon\zeta\right] \\
\|Q_{11}\| &= \frac{1}{3\sqrt{2}}\left[-\sqrt{3}\theta\xi + \sqrt{3}\theta\eta - \varepsilon\xi - \varepsilon\eta + 4\varepsilon\zeta\right] \\
\|Q_{12}\| &= \frac{1}{2\sqrt{3}}\left[\sqrt{3}\xi^2 - \sqrt{3}\eta^2 + 2\theta\varepsilon\right] \\
\|Q_{13}\| &= \frac{1}{2\sqrt{3}}\left[\theta^2 - \varepsilon^2 + \xi^2 + \eta^2 - 2\zeta^2\right] \\
\|Q_{14}\| &= \frac{1}{\sqrt{6}}\left[\sqrt{3}\theta\xi + \sqrt{3}\theta\eta + \varepsilon\xi - \varepsilon\eta\right]
\end{aligned} \tag{17}$$

The iso-stationary function is obtained by inserting these extremal coordinates into Eq. 16. Since the edge distortions were transformed according to the irreps of $\mathbf{S_5}$, the iso-stationary function naturally decomposes into three independent terms, one for each irrep.

$$\begin{aligned}\|E\| &= \|E\|_{G_1}+\|E\|_{H_1}+\|E\|_{H_2}\\ &= -\frac{16}{45}f_1-\frac{1}{9}f_1-\frac{1}{3}f_3 = E^{JT}_{G_1}f_1+\frac{5}{4}E^{JT}_{H_1}f_1+\frac{5}{4}E^{JT}_{H_2}f_3\\ &= -\frac{8}{35}+\frac{1}{21}(f_1-f_3) = E^0+E^1(f_1-f_3)\end{aligned} \tag{18}$$

where f_1 and f_3 are fourth-order polynomials in the c-coordinates:

$$\begin{aligned}f_1 =& \frac{3}{8}\left(\theta^2+\varepsilon^2\right)^2+\frac{1}{6}\left(\xi^2+\eta^2+\zeta^2\right)^2\\ &+\frac{1}{3}\left(\theta^2+\varepsilon^2\right)\left(\xi^2+\eta^2+\zeta^2\right)+\frac{5}{6}\left(\xi^2\eta^2+\eta^2\zeta^2+\zeta^2\xi^2\right)\\ &+\frac{5}{12}\left(\theta^2-\varepsilon^2\right)\left(2\zeta^2-\eta^2-\xi^2\right)-\frac{5}{2\sqrt{3}}\theta\varepsilon\left(\xi^2-\eta^2\right)\\ f_3 =& \frac{1}{8}\left(\theta^2+\varepsilon^2\right)^2+\frac{1}{2}\left(\xi^2+\eta^2+\zeta^2\right)^2\\ &+\left(\theta^2+\varepsilon^2\right)\left(\xi^2+\eta^2+\zeta^2\right)-\frac{3}{2}\left(\xi^2\eta^2+\eta^2\zeta^2+\zeta^2\xi^2\right)\\ &-\frac{3}{4}\left(\theta^2-\varepsilon^2\right)\left(2\zeta^2-\eta^2-\xi^2\right)+\frac{3\sqrt{3}}{2}\theta\varepsilon\left(\xi^2-\eta^2\right)\end{aligned} \tag{19}$$

Although the current JT graph exhibits the instability of a fivefold degenerate level within $\mathbf{S_5}$ symmetry, its iso-stationary function exactly mimics that of the icosahedral quintuplet in the $H\otimes(g+2h)$ JT problem [13], with the sole difference that in the present case the JT stabilization energies are no longer free parameters but are defined by the connectivity of the graph. The correspondence with the icosahedral symmetry group is explained by the permutational nature of the icosahedral fivefold representation. The exact values of these JT stabilization energies (in units of γ^2) are easily retrieved from the expressions in Eq. 18.

$$\begin{aligned}E^{JT}_{G_1} &= E^{JT}_{G} = -16/45\\ E^{JT}_{H_1} &= E^{JT}_{Ha} = -4/45\\ E^{JT}_{H_2} &= E^{JT}_{Hb} = -12/45\end{aligned} \tag{20}$$

The extremal structure of the iso-stationary function has been extensively studied, and it was shown that the nature of the extrema depends on the exact values of the $E^{JT}_G, E^{JT}_{Ha}, E^{JT}_{Hb}$ parameters [13]. At present we shall not list all stationary points but shall instead limit ourselves to the ones corresponding with the absolute minima, providing in Table 6, energy, symmetry, and Hessian eigenvalues of the global minima (α orbit) and the transition states connecting these minima (γ orbit). Under the current regime ($E^1>0$), six equivalent pentagonal minima can be identified, forming the α orbit of Table 6. All these minima are equidistant in Q-space, and tunneling between all of them is equally probable and is mediated by the fifteen saddle points of the γ orbit. In this way, the topology of the dynamic JT system can be represented by the complete graph on six vertices with the vertices denoting the six $\mathbf{D_5}$ minima and the edges the fifteen tunneling pathways. The edge distortions leading to the α_2 minimum are shown in Fig. 3.

The rich topology of this tunneling graph results in closed cycles of lengths from three to six [15, 16]. Phase tracking in Q-space shows that all closed paths of length three give rise to a Berry phase of π [17]. Since these triangles form a basis for the cycle space of the graph, all other cycles can always be written as a sum of these three-cycles and their Berry phases will be equal to the sum of the Berry phases of the three-cycles involved, modulo 2π. As an example, the four-cycle (α_1–α_2–α_3–α_4) can be decomposed into the two three-cycles (α_1–α_2–α_4) and (α_2–α_3–α_4). Consequently, this four-cycle will have a Berry phase of ($\pi+\pi$) mod $2\pi=0$. In the current case, where all three-cycles carry a Berry phase of π, one can simply state that all odd cycles will have a Berry phase of π, while all even cycles will carry a Berry phase of zero. A special feature of the icosahedral point group is that the direct square of the quintuplet representation contains the H representation twice, giving rise to a product multiplicity of two H-modes in the corresponding JT problem: $H\otimes(g+2h)$. This was solved previously by orthogonalization of the coupling coefficients [18]. The resulting couplings were labeled as H_a and H_b. It was later shown that this somewhat arbitrary multiplicity separation coincided with a different parentage in the $\mathbf{S_6}$ covering group [4, 19]. This also provided extra selection rules for several matrix elements. At present we see that the parent $\mathbf{S_5}$ group also provides a natural product separation as H_1 and H_2, which, moreover, also coincides with H_a and H_b. This is explained by the fact that the embedding of the icosahedral group in the complete 6-graph, K_6, contains $\mathbf{S_5}$ as an intermediate subgroup:

$$\mathbf{S}_6 \rightarrow \mathbf{S}_5 \rightarrow \mathbf{I}. \tag{21}$$

5 The 20-vertex graph and the sixfold degeneracy

The group $\mathbf{S_5}$ contains one sextuplet representation which in $\mathbf{A_5}$ splits into two triplets, labeled as the icosahedral T_1 and T_2 irreps. Clearly, since the icosahedral group cannot act transitively on a set of seven elements, we should not expect that it can host a sixfold degeneracy. In the context of the graph-theoretical JT theorem, this makes these triplets exceptional, since they cannot be related to the

Table 6 Energy, symmetry, and Hessian eigenvalues of the global minima (α orbit) and the transition states connecting these minima (γ orbit)

Orbit	Dim	Sym	Eigenvectors $(\theta, \varepsilon, \xi, \eta, \zeta)$	Energy	Hessian eigenvalues
α	6	$\mathbf{D_5}$	$\alpha_{1,2} = \frac{1}{\sqrt{10}}\left(\sqrt{3}, 1, \pm\sqrt{6}, 0, 0\right)$ $\alpha_{3,4} = \frac{1}{\sqrt{10}}\left(\sqrt{3}, -1, 0, \pm\sqrt{6}, 0\right)$ $\alpha_{5,6} = \frac{1}{\sqrt{5}}\left(0, \sqrt{2}, 0, 0, \pm\sqrt{3}\right)$	$E^{JT}_{(2^2,1)} = -4/15 = -36/135$	$\frac{4}{15}, \frac{4}{15}, \frac{4}{15}, \frac{4}{15}$
γ	15	$\mathbf{D_2}$	$(0,0,1,0,0)$ $(0,0,0,1,0)$ $(0,0,0,0,1)$ $\frac{1}{\sqrt{8}}\left(1, \sqrt{3}, \sqrt{2}, 0, \pm\sqrt{2}\right)$ $\frac{1}{\sqrt{8}}\left(1, \sqrt{3}, -\sqrt{2}, 0, \pm\sqrt{2}\right)$ $\frac{1}{\sqrt{8}}\left(1, -\sqrt{3}, 0, \sqrt{2}, \pm\sqrt{2}\right)$ $\frac{1}{\sqrt{8}}\left(1, -\sqrt{3}, 0, -\sqrt{2}, \pm\sqrt{2}\right)$ $\frac{1}{2}\left(\sqrt{2}, 0, 1, \pm 1, 0\right)$ $\frac{1}{2}\left(\sqrt{2}, 0, -1, \pm 1, 0\right)$	$\left(4E^{JT}_{(4,1)} + 5E^{JT}_{(3,2)} + 15E^{JT}_{(2^2,1)}\right)/24 = -33/135$	$-\frac{2}{9}, \frac{2}{9}, \frac{2}{9}, \frac{2}{9}$

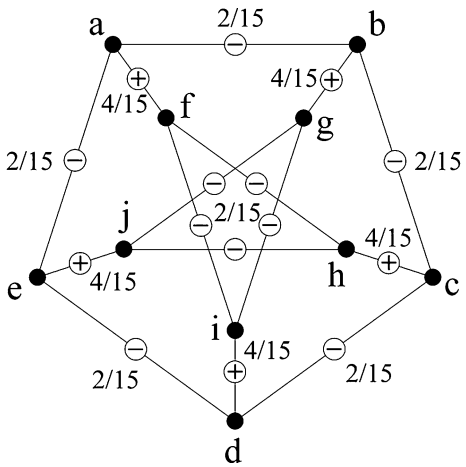

Fig. 3 Edge distortions of the Petersen graph leading to the α_2 minimum in the $H_1 \otimes (G_1 + H_1 + H_2)$ problem

embedding of a maximal subgroup of the icosahedral group. However, there exists an interesting relationship between both triplets, which points to a common sextuplet ancestor. The characters of the two T irreps are the same, except for the sign of the $\sqrt{5}$ (see Table 1). Such a pair of representations—which have opposite signs only for the irrational number appearing in their transformations—are known as irrational conjugates. As a result, the Clebsch-Gordan coupling coefficients for direct products involving these T states are likewise related [18]. These relationships may be used to explain some intriguing degeneracies in the multiplet terms, based on the icosahedral H and G shells. For some configurations, the T_1 and T_2 terms occur in pairs, with degenerate Coulomb energies [20, 21]. To explain these regularities, Judd and Lo have introduced a so-called kaleidoscopic operator that permutes the two triplets [22, 23]. In view of this conjugation between the two triplets, it is worthwhile to examine a model of JT activity in a sextuplet level of a graph with $\mathbf{S_5}$ symmetry. The 20-graph in Fig. 1c provides such a model. In this model an unexpected symmetry selection rule appears, which prevents the JT splitting of the sextuplet into two triplets.

The spectrum of the 20-graph is $\left\{4, 3^4, 0^5, (-2)^6, (-1)^4\right\}$. If each node were occupied by one electron, a closed shell would be obtained. Adding an extra electron would then give rise to a sixfold degenerate JT instability. It is possibly noteworthy that the eigenvectors of the sextuplet roots can be obtained in a special monomial form, with the same weight on each vertex. To this end, we use the embedding of a maximal subgroup of order 20, known as the Frobenius group, which is a meta-cyclic group containing one C_5-axis and five C_4-axes [24]. The intersection of this group with $\mathbf{I}$ is the pentagonal subgroup $\mathbf{D_5}$. Its character table is displayed in Table 7, and the subduction relations from $\mathbf{S_5}$ are as follows:

Table 7 Character table for the meta-cyclic MC5-4 Frobenius group, and the $\mathbf{S_5}$ cycle structure

	E $\{1^5\}$	$4C_5$ $\{5\}$	$5C_2$ $\{1,2^2\}$	$5C_4$ $\{1,4\}$	$5C_4^3$ $\{1,4\}$
A	1	1	1	1	1
B	1	1	1	−1	−1
Γ_1	1	1	−1	i	−i
Γ_2	1	1	−1	−i	i
G	4	−1	0	0	0

$$
\begin{aligned}
A_1 &\rightarrow A \\
A_2 &\rightarrow B \\
G_1 &\rightarrow G \\
G_2 &\rightarrow G \\
H_1 &\rightarrow B + G \\
H_2 &\rightarrow A + G \\
I &\rightarrow \Gamma_1 + \Gamma_2 + G
\end{aligned}
\tag{22}
$$

We note that the complex conjugate non-degenerate irreps, Γ_1 and Γ_2, directly generate the sextuplet representation. According to induction theory, this process will yield at once the six eigenvectors in monomial form [25], where we use the sixfold axis as cyclic coset generator.

One of the eigenvectors is shown in Fig. 4. The five others may be obtained by acting on this with the sixfold generator specified in Table 3. The symmetrized square of the I representation can be obtained with the expression in Eq. 5, and reads:

$$[I \otimes I] = A_1 + A_2 + G_1 + 2H_1 + H_2 \tag{23}$$

On the other hand, the representations of the edge distortions can be obtained separately for each edge orbit, and they read:

$$
\begin{aligned}
\Gamma_{10}(e) &= A_1 + G_1 + H_1 \\
\Gamma_{30}(e) &= A_1 + 2G_1 + 2H_1 + H_2 + I
\end{aligned}
\tag{24}
$$

When comparing the required JT modes in Eq. 23 with the available edge distortions in Eq. 24, it is observed that one of the JT modes, viz., the A_2, is missing from the space of the edge distortions. The vertex representation likewise does not contain this symmetry, so changes of vertex weights cannot provide such a symmetry breaking, either. On the other hand, the distortion space contains an I symmetry mode, which is not JT active. The latter case is not uncommon in the molecular JT effect, but the fact that one of the JT modes is missing is exceptional. In molecules this does not occur, except for the special case of linear molecules, which are JT inactive. In fact, these are the only exceptions to the JT effect in 3D space. On the other hand, when considering structures in higher-dimensional spaces, such as the hyper-octahedron, it happens that not all JT modes have counterparts in the hyperspace of the nuclear distortions [2]. From our present perspective, the absence of the A_2 mode is particularly intriguing since this mode breaks the $\mathbf{S_5}$ symmetry to $\mathbf{A_5}$, and its only effect on the representations is to split the sextuplet into two triplets:

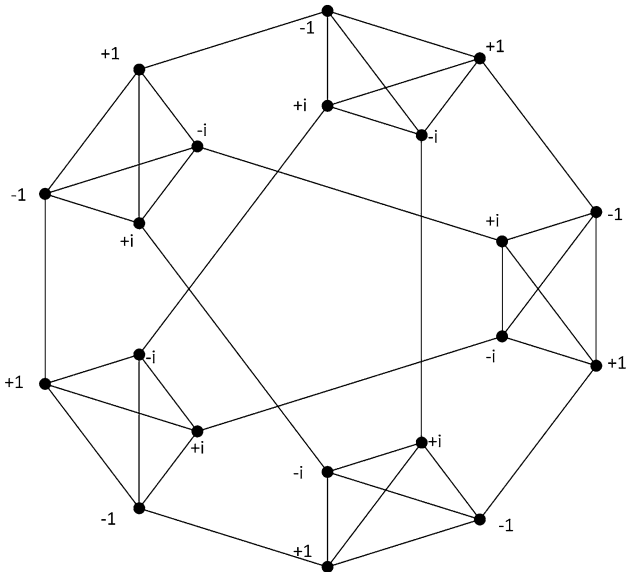

Fig. 4 Eigenvector of the sextuplet manifold in the 20-graph. The other components may be obtained by cyclic permutations under the $\{2,3^2,6^2\}$ operator of Table 3

$$I \rightarrow T_1 + T_2 \tag{25}$$

In fact, this branching provides the operator form for the A_2 mode. If we again work out the symmetrized square of the I irrep in the $\mathbf{A_5}$ subgroup, Eq. 23 becomes:

$$
\begin{aligned}
[I \otimes I] &= [(T_1 + T_2) \otimes (T_1 + T_2)] \\
&= [T_1 \otimes T_1] + [T_2 \otimes T_2] + T_1 \otimes T_2
\end{aligned}
\tag{26}
$$

The two T squares in the right-hand side of Eq. 26 both yield an A, which corresponds to the presence of two A-quantities in Eq. 23, but the symmetrized square of I can yield only one totally symmetric A_1, which will correspond to the trace of the sextuplet. The other A-quantity thus must be an A_2. This operator will be equal to the difference of the trace-operators for T_1 and T_2, which is precisely the operator that splits I into T_1 and T_2. The absence of such a mode in the distortion space leads us to the conclusion that, in this 20-graph, there is no distortion that can produce a neat separation of the two conjugate triplets. The only distortion that will partially distinguish both triplets is a distortion to $\mathbf{D_5}$ symmetry, using a component of the H representation, with the following subduction relation:

$$I \rightarrow \begin{cases} T_1 \rightarrow A_2 + E_1 \\ T_2 \rightarrow A_2 + E_2 \end{cases} \quad (27)$$

In this case, the E-components are resolved as E_1 and E_2 under the C_5-axis, but the non-degenerate level is the same for both triplets.

6 Conclusions

In this paper we have investigated three graphs with $\mathbf{S_5}$ symmetry as models for JT activity in icosahedral molecular problems. Such graph models can be used as pseudo-particle models of actual Jahn–Teller problems, the connection being based on the link between the automorphism group of the graph and the molecular symmetry group. In the case of the fivefold degenerate representation, the JT problem is characterized by a product multiplicity problem. Previous solutions of this were based on spherical symmetry and induction theory, as well as on subduction relations from the symmetric $\mathbf{S_6}$ groups. The present analysis shows that the intermediate $\mathbf{S_5}$ group is sufficient to obtain the same multiplicity resolution. From the graph-theoretical perspective, a further interesting feature was found in that the symmetry breaking of the sextuplet level into two triplets requires a pseudo-scalar operator, leading from $\mathbf{S_5}$ to $\mathbf{A_5}$, which was, however, absent from the edge-weight distortion space. This selection rule might provide a justification for the validity of Judd's 'kaleidoscopic' operator [22, 23]. It will also be interesting to examine the combined $(T_1 \oplus T_2)$ pseudo-JT problem. So far, only the $(T_{1g} \oplus T_{1u})$ adiabatic potential has been investigated [26].

Clearly, the graph-theoretical JT-conjecture must further be refined, since the last case shows that selection rules may prevent some modes of symmetry breaking by edge distortions. In which graphs this occurs, and why, are open questions.

Acknowledgments Financial support from the Flemish Science Foundation (FWO) is gratefully acknowledged. The work of TP has been partially financed by ARRS project P1—0294 and project N1—0011 within the EUROCORES Programme EUROGIGA (project GReGAS) of the European Science Foundation.

References

1. Bersuker IB, Polinger VZ (1989) Vibronic interactions in molecules and crystals. Springer, Berlin
2. Ceulemans A, Lijnen E (2010) Electronic degeneracy and vibrational degrees of freedom: the permutational proof of the Jahn–Teller theorem. In: Köppel H, Yarkony DR, Barentzen H (eds) The Jahn–Teller effect. Springer, Heidelberg, pp 25–50
3. Trinajstić N (1992) Chemical graph theory, 2nd edn. CRC Press, Boca Raton
4. Ceulemans A, Lijnen E, Fowler PW, Mallion RB, Pisanski T (2012) Graph theory and the Jahn–Teller theorem. Proc Roy Soc A 468:971–989
5. Fowler PW (2003) Symmetry aspects of distortivity in π systems. In: Ceulemans A, Chibotaru LF, Kryachko E (eds) Advances in quantum chemistry, vol 44. Elsevier, Amsterdam, pp 219–237
6. Pauncz R (1995) The symmetric group in quantum chemistry. CRC Press, Boca Raton
7. Pisanski T. If a graph G has n vertices, then the extension, defined as THE(G), has $n*n$-n vertices. Namely, the vertices of THE(G) are ordered pairs of distinct vertices of G. If u and v are adjacent vertices of G then uv is adjacent to vu and for any other vertex w from G, different from u and v, the vertex uw is adjacent to uv (to be published)
8. Griffith JS (1961) The theory of transition-metal ions. Cambridge University Press, Cambridge
9. Ceulemans A, Fowler PW (1989) SO(4) symmetry and the static Jahn–Teller effect in icosahedral molecules. Phys Rev A 39:481–493
10. Ceulemans A, Lijnen E (2007) The Jahn–Teller effect in chemistry. Bull Chem Soc Jpn 80:1229–1240
11. Boyle LL, Parker YM (1980) Symmetry coordinates and vibration frequencies for an icosahedral cage. Mol Phys 39:95–109
12. Moate CP, O'Brien MCM, Dunn JL, Bates CA, Liu YM, Polinger VZ (1996) $H \otimes h$: a Jahn–Teller coupling that really does reduce the degeneracy of the ground state. Phys Rev Lett 77:4362–4365
13. Ceulemans A, Fowler PW (1990) The Jahn–Teller instability of fivefold degenerate states in icosahedral molecules. J Chem Phys 93:1221–1234
14. Ceulemans A (1987) The structure of Jahn–Teller surfaces. J Chem Phys 87:5374–5385
15. Ceulemans A, Lijnen E (2005) Berry phase and entanglement in the icosahedral $H \otimes (g \oplus 2\ h)$ Jahn–Teller system with trigonal minima. Phys Rev B 71:014305
16. Manini N, De Los Rios P (2000) Berry phase and ground-state symmetry in $H \otimes h$ dynamical Jahn–Teller systems. Phys Rev B 62:29–32
17. Berry MV (1984) Quantal phase factors accompanying adiabatic changes. Proc Roy Soc A 392:45–57
18. Fowler PW, Ceulemans A (1985) Symmetry relations in the property surfaces of icosahedral molecules. Mol Phys 54:767–785
19. Lijnen E, Ceulemans A (2007) The permutational symmetry of the icosahedral orbital quintuplet and its implication for vibronic interactions. Europhys Lett 80:67006
20. Plakhutin BN, Carbó-Dorca R (2000) Icosahedral symmetry structures with open-shell electronic configuration h^N ($N = 1$–9). Phys Lett A 267:370–378
21. Plakhutin BN, Arbuznikov AV (1997) Spectrum of states in icosahedral structures with g^N electronic configuration ($N = 1$–7). 2. Ab initio calculation of the C20 (Ih) molecule and its anions. J Struct Chem 38:501–510
22. Judd BR, Lo E (1999) Coulomb energies of icosahedral h orbitals. J Chem Phys 111:5706–5729
23. Lo E, Judd BR (1999) Implications of non-feasible transformations among icosahedral h orbitals. Phys Rev Lett 82:3224–3227
24. Voskresenskaya GV (2000) Metacyclic groups and modular forms. Math Notes 67:129–137
25. Ceulemans A, Beyens D (1983) Monomial representation of point-group symmetries. Phys Rev A 27:621–631
26. Ceulemans A, Chibotaru LF (1996) Icosahedral $T_{1u} + T_{1g}$ Jahn–Teller problem. Phys Rev B 53:2460–2462